

H1prelim-22-032, submitted to the DIS2022 conference
Date: June 29, 2022

Probing hadronization using leading particles and leading substructures of jets at HERA

H1 Collaboration

Abstract

We measure the charge and momentum correlations of the two leading particles in a jet in terms of momentum along the jet axis. The observable, r_c used is expected to be very sensitive to fragmentation dynamics. The r_c measured in various kinematic variables and in particular the formation time (t_{form}) brings the information of when the di-hadron fragmentation occurred. Formation time can separate the regions whether the fragmentation is dominated by perturbative or non-perturbative dynamics. The associated structure in jet in terms of partonic branching is studied via jet substructure and recursive soft drop used to trace back the C/A decluster tree. An association of subjects to the leading particles and the related correlations is framed to extract r_c which is more resembles as partonic proxies. It is revealing that soft and core part of the fragmentation significantly differ in r_c correlations in specific kinematic region.

Contents

1	Introduction: Observable	1
2	Kinematic variables	2
3	Data and MC samples and event selection	2
4	Jet reconstructions	3
4.1	Recursive soft drop	3
4.1.1	Recursive soft drop: resolved prongs	4
5	Results and key plots	5
5.1	Jet properties and data and MC comparison	5
5.2	Constituents in jets	6
5.3	Some distributions related to sub-jets	7
5.4	Key plots	9

1 Introduction: Observable

In the process of fragmentation the two-particle correlation of the leading charged hadron h_1 and next-to-leading charged hadron h_2 is studied with charge correlations [1, 2]. The charge correlation ratio, r_c , is defined from the differential cross sections $d\sigma_{h_1 h_2}/dX$ to quantify flavor and kinematic dependence of hadronization in the production of h_1 and h_2 or \bar{h}_2 (the anti-particle of h_2),

$$r_c(X) = \frac{d\sigma_{h_1 h_2}/dX - d\sigma_{h_1 \bar{h}_2}/dX}{d\sigma_{h_1 h_2}/dX + d\sigma_{h_1 \bar{h}_2}/dX} . \quad (1)$$

We will explore the dependence of r_c on a variety of kinematic variables, X . In the definition, Eq. (1), h_1 and h_2 can in principle be arbitrary hadron species, including charged and neutral hadrons. We will select the events only in the case where both of them are charged particles. The r_c is negative for the cases where $h_1 \bar{h}_2$ cases dominate over $h_1 h_2$ and in the string breaking picture opposite pair production dominates that leads to r_c value be between 0 and -1 .

2 Kinematic variables

Formation time, $t_{\text{form}} = \frac{[2z(1-z)P]}{k_{\perp}^2}$, is calculated from leading (L) and next-to-leading (NL) particle's kinematics. Leading and next-to-leading particles are selected in terms of the momentum fraction along the jet axis. In formulating the formation time, z and P are defined as follows $z = P_{\text{NL}}/(P_{\text{NL}} + P_{\text{L}})$, $P_{\text{L}} = (1-z)P$ and $P_{\text{NL}} = zP$. Formation time can be related to time scale of correlations between the two leading particles. Small formation time corresponds small z or large k_{\perp} . For a specific z (specific P_{NL} and P_{L} magnitude), a large θ or large k_{\perp} corresponds to a small t_{form} . This is the region where early de-correlations take place resulting in small formation time. This small z region can be physically thought of wide angle gluon radiations. On the contrary a small θ corresponds to small k_{\perp} and this is the region for large t_{form} .

When we calculate formation time with prongs where the kinematics of the prongs and charge of the prongs are used. The charge of a prong is taken as the charge of the leading particle. This way of representation would give more resemblance to partonic picture evolution of a hard scattered partons to the final state particles.

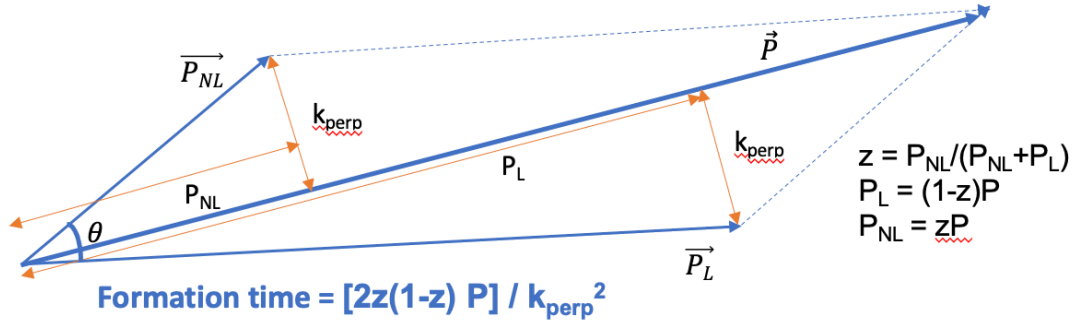


Figure 1: Leading (L) and Next-Leading (NL) particle and formation time definition.

3 Data and MC samples and event selection

The data taken by the H1 experiment during 2003-2007 using 27.6 GeV electron/positron scatters off 920 GeV proton at HERA, which corresponds to a center-of-mass energy $\sqrt{s} = 319$ GeV. The data are selected requiring functional central trackers (CJC1, CJC2) and calorimeters (LAr, SpaCal). The MC samples are reconstructed using the same detector condition of the corresponding years with Djangoh 1.4 and Rapgap 3.1 event generator. Subtrigger ST67 is used while subtrigger ST77 ($\sim 1\%$) is rejected for this analysis. This subtrigger is sufficient for our interest in getting relatively high Q^2 (> 150 GeV²) events and with good tracking using central detectors.

The z -vertex distribution spreads widely mostly due to the 107 colliding bunch size in the accelerator while the transverse spread is narrow. The interaction region in the z direction in this analysis is required to be less than ± 30 cm.

The longitudinal momentum of Hadronic Final State (HFS) and the scattered electron ($E - p_z$) is expected to be two times the incident electron energy, i.e., 55.2 GeV. The spread in the variable ($E - p_z$) appears due to experimental resolution effects in determination of HFS and photon radiations from colliding beam. We have taken events with $45 < E - p_z < 65$ GeV and this reduces events with initial state photon radiations and photoproduction events.

To have a well defined kinematics the events are selected with $Q^2 > 150 \text{ GeV}^2$ and $0.2 < y < 0.7$.

4 Jet reconstructions

Jets are reconstructed from HFS with $p_T > 0.2 \text{ GeV}$ using the lab frame with jet $p_T > 5 \text{ GeV}$. The fiducial cuts in jet pseudorapidity is $-1.5 < \eta < 1.5$. Jets are reconstructed with fastjet anti-kt algorithm with $R = 1.0$ with energy weighted scheme. For the simplicity we are currently using only leading p_T jet which dominates about 75% of cases. Two jets in events might be interesting in terms of origin from higher order processes and in such a case the analysis would be interesting in predicting r_c which might be dominated by jets of gluonic origin.

The analysis requires the leading momentum objects (subjects) within jets to have well defined charge either +1 or -1. The charge of the subjects are currently picked from the charge of the leading constituents.

The tracks are selected using the class H1PartSelTrack with defined “primary” confined for “central” tracks. This is the major part where the event sample gets reduced for the analysis. The selection criteria for the tracks is supposed to give very well defined tracks in the central region.

4.1 Recursive soft drop

In the Soft Drop (SD) [4] [3] procedure the constituents of an initial jet with radius R_0 is re-clustered with the Cambridge/Aachen (C/A) algorithm. The soft wide angle emissions are removed that do not satisfy the SD condition. This is a powerful probe of the QCD splitting function. We introduce a recursive extension [5] of the SD algorithm —aptly named Recursive Soft Drop (RSD)— where SD is reapplied along the C/A clustering history until a specified number n of SD conditions have been satisfied. The number $n = 1$ corresponds to first split while $n = 2$ would correspond to the second split. The place where we will stop here when the leading and next-to leading particles are found in two separate branches or prong. We will call them resolved prongs n_R . This way of tagging would essentially control nonoperative aspects of splitting fractions. Fastjet has the contributory components, the recursive soft drop algorithm, [RecursiveTools 2.0.1 2021-08-21](#), is used.

Defining z_g and R_g as

$$z_g = \frac{\min(p_{t,1}, p_{t,2})}{p_{t,1} + p_{t,2}} > z_{\text{cut}} \left(\frac{R_g}{R_0} \right)^\beta, \quad (2)$$

$$R_g = \Delta R_{12} = \sqrt{\Delta\eta_{1,2}^2 + \Delta\phi_{1,2}^2}, \quad (3)$$

the values for the $\beta = 1$ and $z_{\text{cut}} = 0.2$ is used in the main analysis. $\beta = 1$ means that grooming using the dynamic radius in reaching successive steps and higher z_{cut} means more harsher cuts on soft particles.

In general it is very informative to see the n_R distributions to check where the correlation of the prongs and leading particles happens. Specifically z_{cut} has much to do in transforming N_R distributions. Larger z_{cut} eliminates soft wide angle radiations and the matching probability of the leading hadron gets enhanced in the first node. Nevertheless, a modest z_{cut} cut would still keep a soft wide angle component in the first split. The consecutive splits are narrower and thus for the current analysis we will split the data into two subsets. One would be 1st prong and the rest would be in the class of 2^{nd+} prongs.

Charge of the prongs: We have not determined the charge of the prongs as conventional jet charge is calculated. We assign the charge of the prong from the charge of the leading momentum of the particle (along the prong axis).

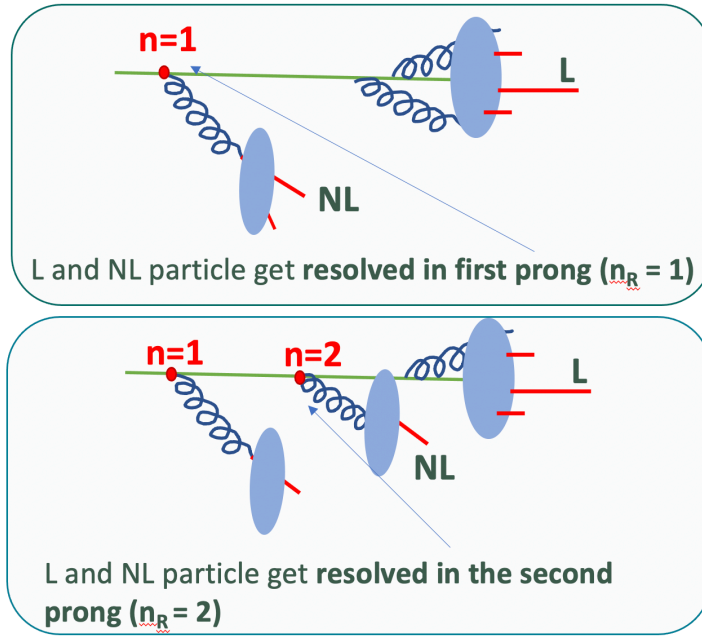


Figure 2: Resolved prongs: the top cartoon shows that the leading and next to leading particles get resolved in the first prong ($n_R = 1$), while the bottom cartoon shows that it needs to go to the second prong to get resolved ($n_R = 2$).

4.1.1 Recursive soft drop: resolved prongs

The kinematics of leading and next-to-leading particles are replaced to that of sub-jets; i.e., the jet with $R = 1.0$ is subdivided into smaller jets mimicking the angular ordering of the shower from the final state particles in jets. Angular order of the branches in the clustering tree is

followed through the hardest branch till the leading hadrons are found in two separate sub-jets. We call at that point that the leading next to leading hadrons are get resolved. Soft drop is used with $z_{\text{cut}} = 0.2$ and $\beta = 1$ in order to remove very soft particles activities surrounding the core hadronization region around the leading particles. In that way we classify the events with $n_R = 1$ (resolved first prong) and $n_R \geq 2$ (resolved 2nd+ prongs). The first split ($n_R = 1$) is relatively wider angle soft splitting and the 2nd+ ($n_R \geq 2$) prongs are relatively narrower and harder splitting.

5 Results and key plots

The r_c is measured in three cases:

- (I) leading charged hadrons in a jet,
- (II) subjets at the first split for the resolved prongs, and
- (II) subjets at the second and further splits for the resolved prongs.

5.1 Jet properties and data and MC comparison

Here the number of jets, jet pseudo-rapidity and jet transverse momentum distributions are plotted.

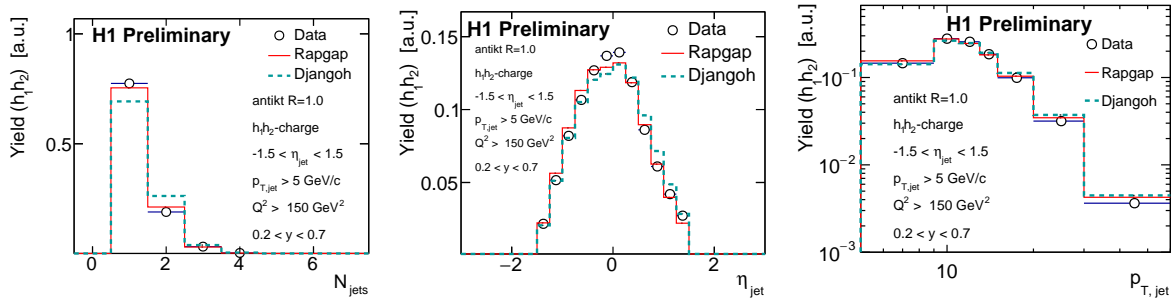


Figure 3: (left) number of jets in an event, (middle) leading jet pseudo-rapidity distributions, (right) leading et transverse momentum distributions. The jet transverse momentum and pseudorapidity regions are indicated. Only the leading jet is considered for the subsequent analysis, corresponding to more than 90% of all jets. The jet rapidity is restricted in order to match the central tracker acceptance for the jet’s leading particle selection. The peak near transverse jet momenta of 10 GeV is a reflection of the $Q^2 > 150$ GeV selection cut.

5.2 Constituents in jets

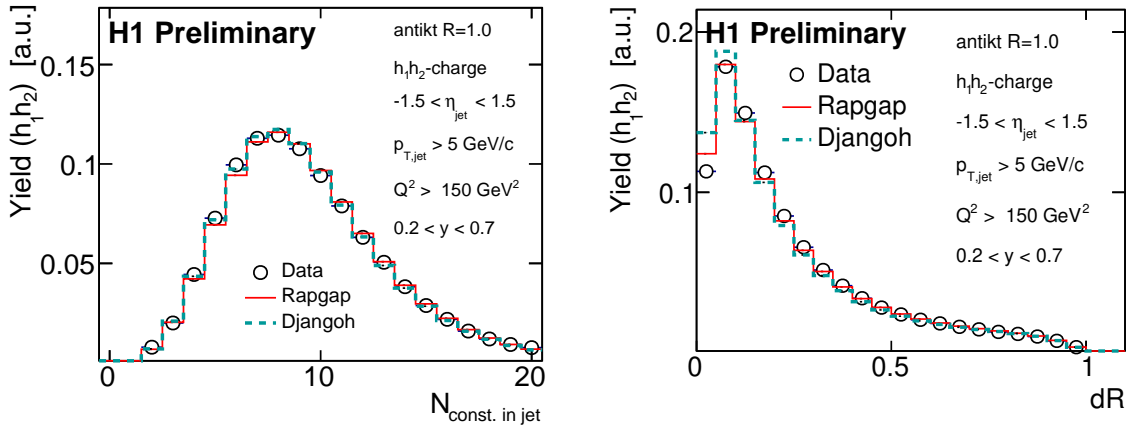


Figure 4: (left) number of constituents, (right) Energy flow within the jet. The number of constituents includes both neutral and charged objects. The distance $dR = \sqrt{(\Delta\eta)^2 + (\Delta\phi)^2}$ is measured with respect to the jet axis.

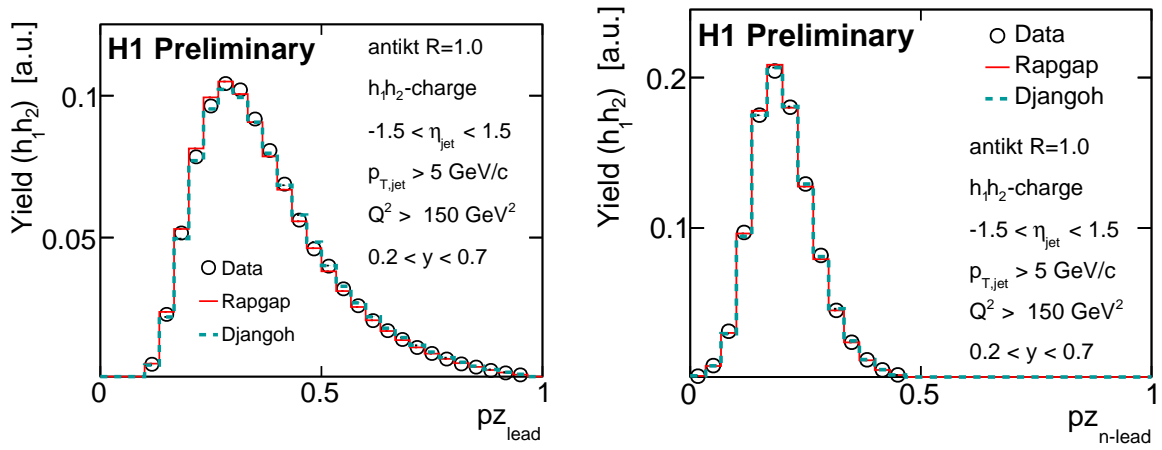


Figure 5: (left) fraction of momentum carried by the leading particle along the jet axis, (right) Fraction of momentum carried by the next to leading particle along the jet axis.

5.3 Some distributions related to sub-jets

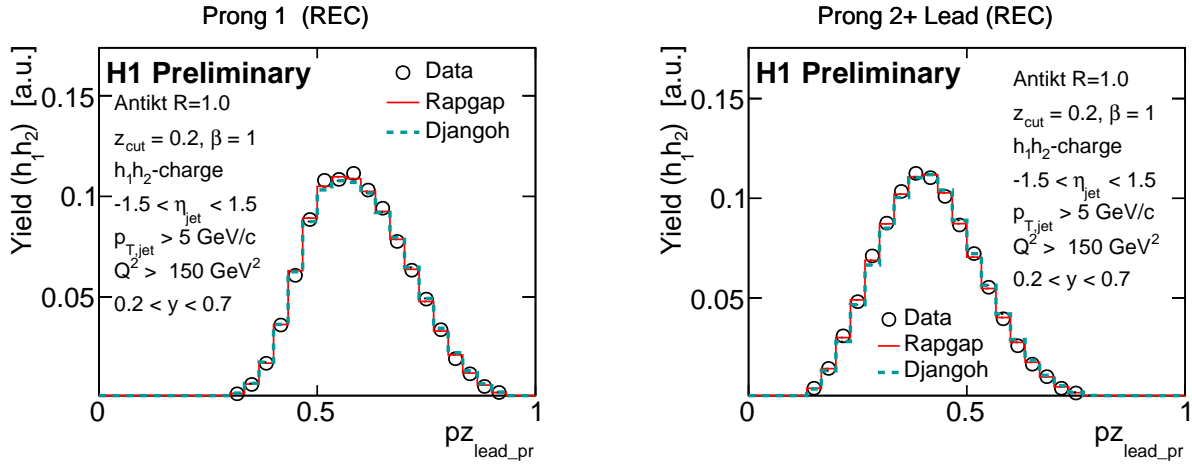


Figure 6: Fraction of momentum carried by the leading jet along the jet axis at the first and the second split.

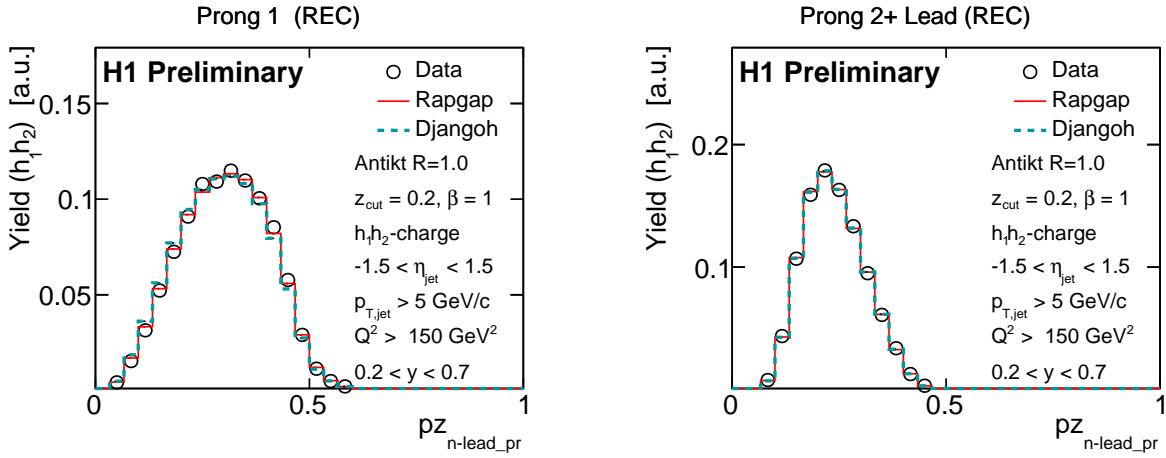


Figure 7: Fraction of momentum carried by the next to leading jet along the jet axis at the first and the second split.

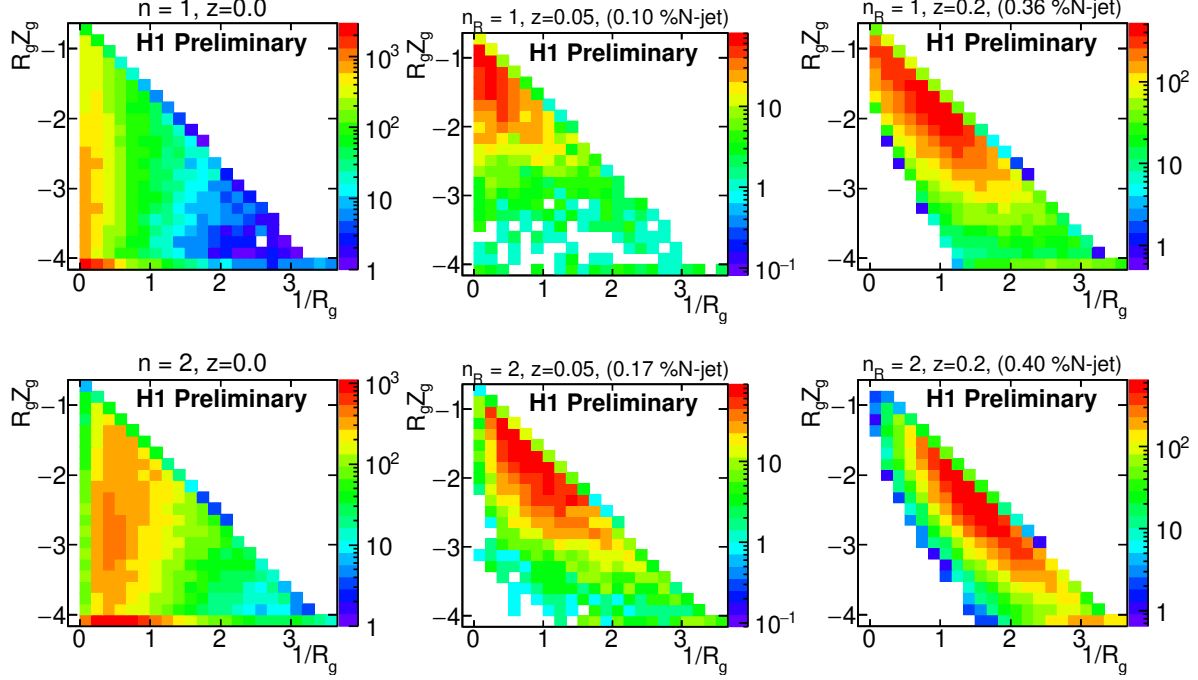


Figure 8: Properties of the recursive soft-drop algorithm, $1/R_g$ vs. $R_g z_g$ at first and second prongs. (left) $z_{\text{cut}} = 0$ and no selection on leading hadrons, (middle and right) leading and next-to-leading hadrons are resolved at $z_{\text{cut}} = 0.05$ and $z_{\text{cut}} = 0.2$, respectively. The $1/R_g$ vs. $R_g z_g$ distributions are shown at the first and second angular ordered splits. The left figure, $n = 1$, is dominated by wide angle soft radiation. At $n = 2$ one observes narrower splits. For $z_{\text{cut}} > 0.05$ and with leading and next-to-leading hadrons resolved, soft radiation is suppressed at the cost of reducing the sample to 10% at $n_R = 1$ and 15% at $n_R = 2$. The highest $z_{\text{cut}} > 0.2$ enhances further the differences between $n_R = 1$ and $n_R > 1$, such that $n_R = 1$ is mostly wide angle soft radiation, whereas $n_R > 1$ is narrow angle harder radiation.

5.4 Key plots

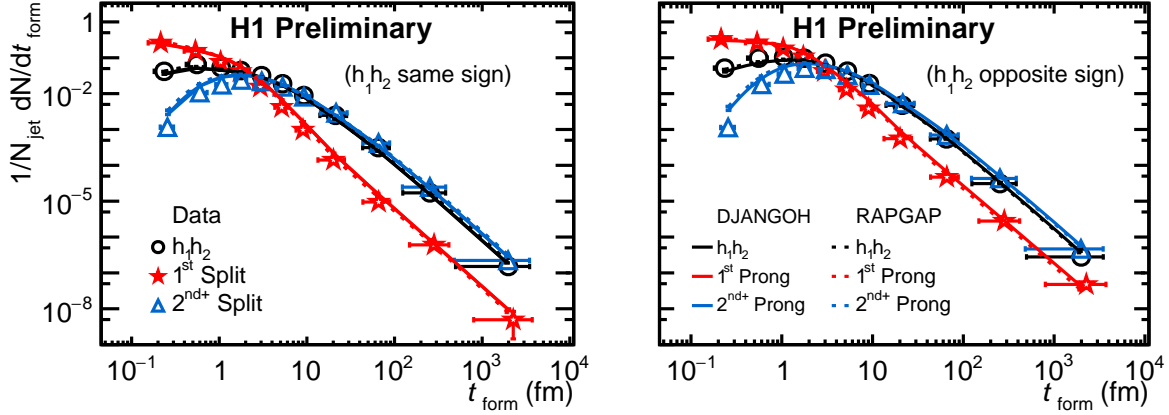


Figure 9: Formation time distributions (t_{form}). The left figure is for the case where the leading hadron (h_1) and the next to leading hadron (h_2) are of same charge and the figure on the right is the case where the leading and the next to leading hadrons have opposite charge. The yield for the case where h_1 and h_2 are of opposite charges is higher compared to the case where h_1 and h_2 are of same charge. The distributions are normalized with the number of jets and the formation time bins. The y -axis represents the density of the charge pairs with formation time. It appears to be that the pair density for first split is more than the subsequent splits and this reflects the fact that the first split is more frequent in earlier time in the parton shower evolution.

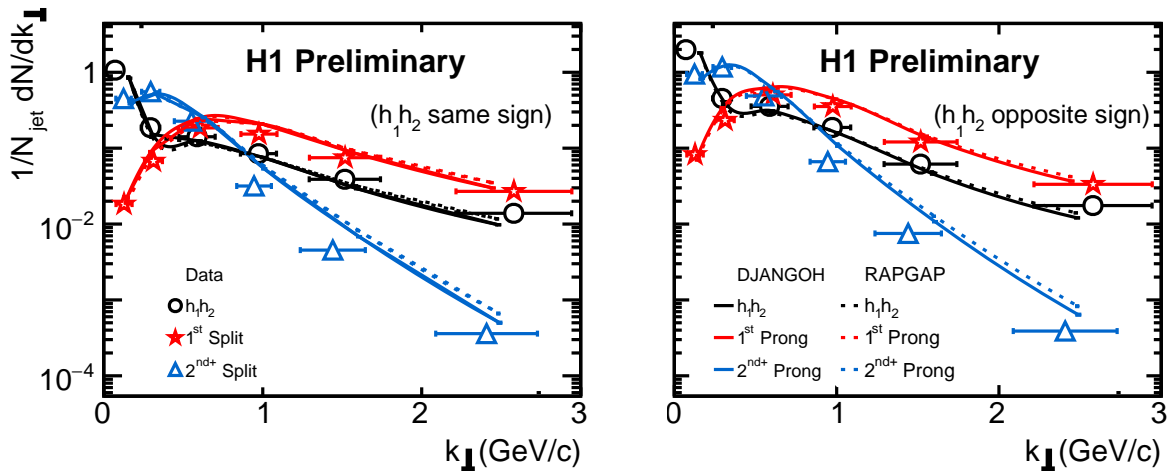


Figure 10: k_{\perp} distributions. The left figure is for the case where the leading hadron (h_1) and the next to leading hadron (h_2) are of same charge and the figure on the right is the case where the leading and the next to leading hadrons have opposite charge.

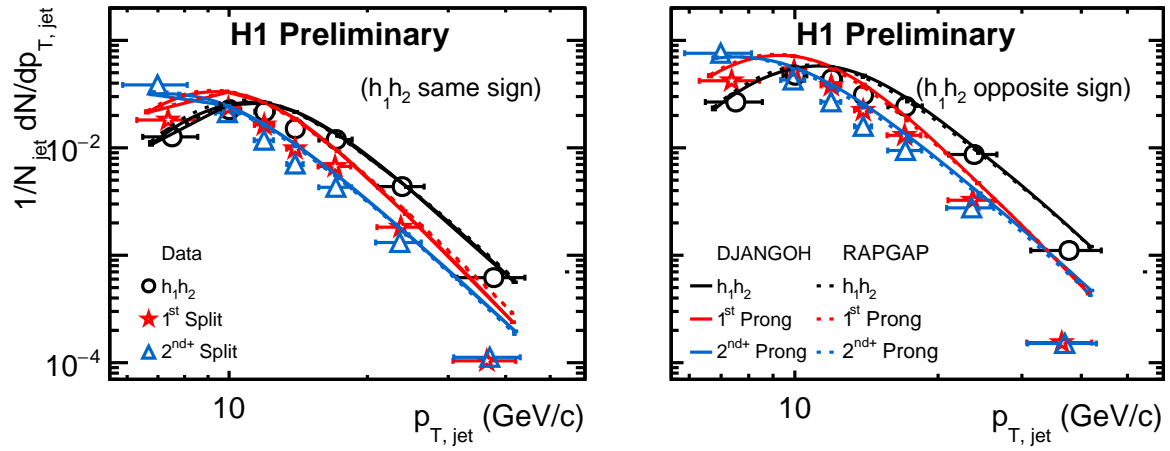


Figure 11: Jet p_T distributions. The left figure is for the case where the leading hadron (h_1) and the next to leading hadron (h_2) are of same charge and the figure on the right is the case where the leading and the next to leading hadrons have opposite charges.

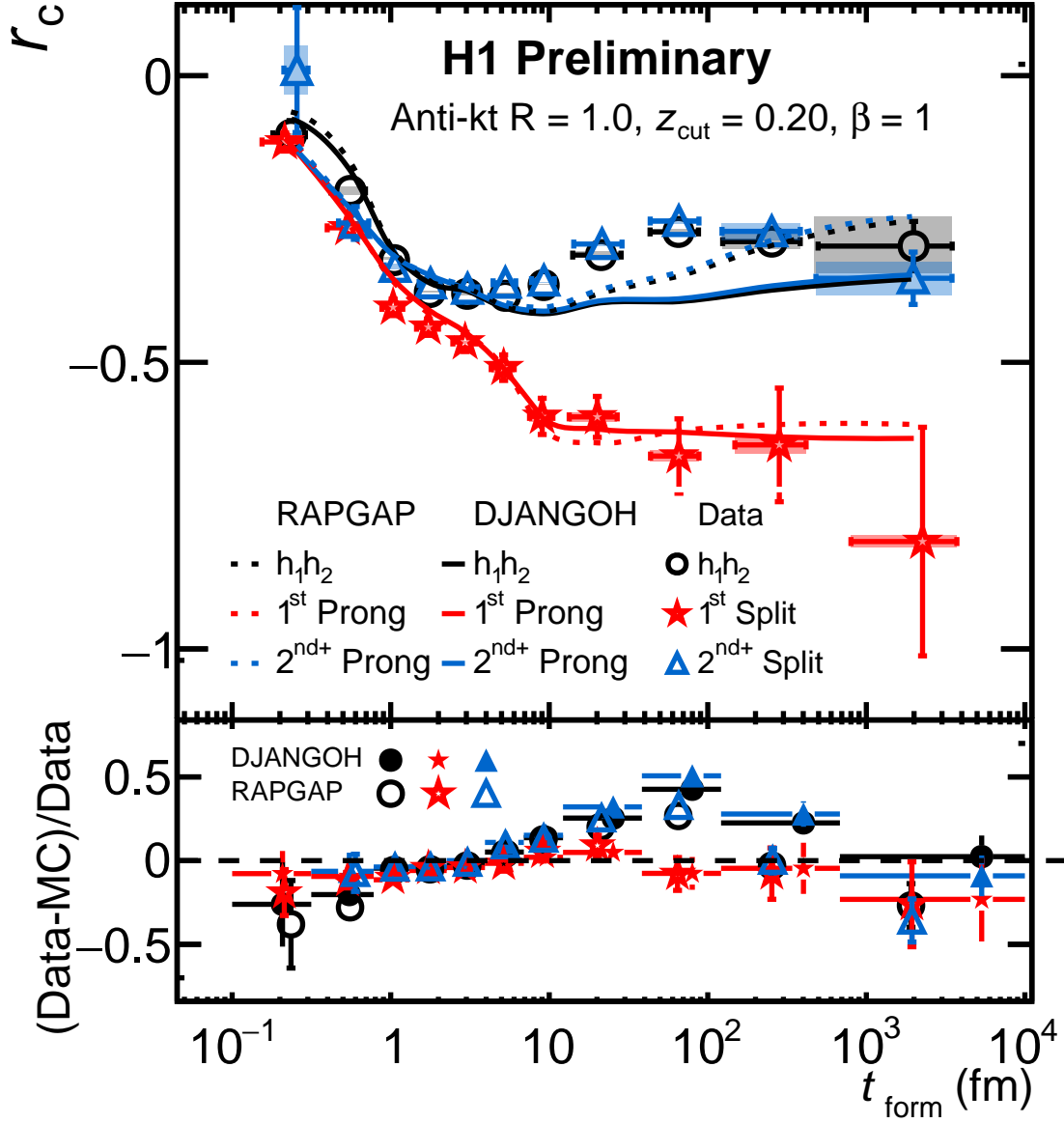


Figure 12: r_c as a function of t_{form} for different splits and $h_1 h_2$. The r_c at small formation time (~ 1 fm) are large k_{\perp} or small z origin, and this is the region where leading and next to leading particles originate from early decorrelations. This region appears to be purely perturbative in nature. Large formation time (~ 10 fm or more) corresponds to nonperturbative in nature where $k_{\perp} < 200$ MeV. The striking difference is that at large formation time r_c for the first split is stronger compared to that of the subsequent splits. Djangoh and Rapgap compare with data fairly well in most of the region. The systematic bands are the errors appearing from bin-by-bin corrections using Rapgap and Djangoh event generators.

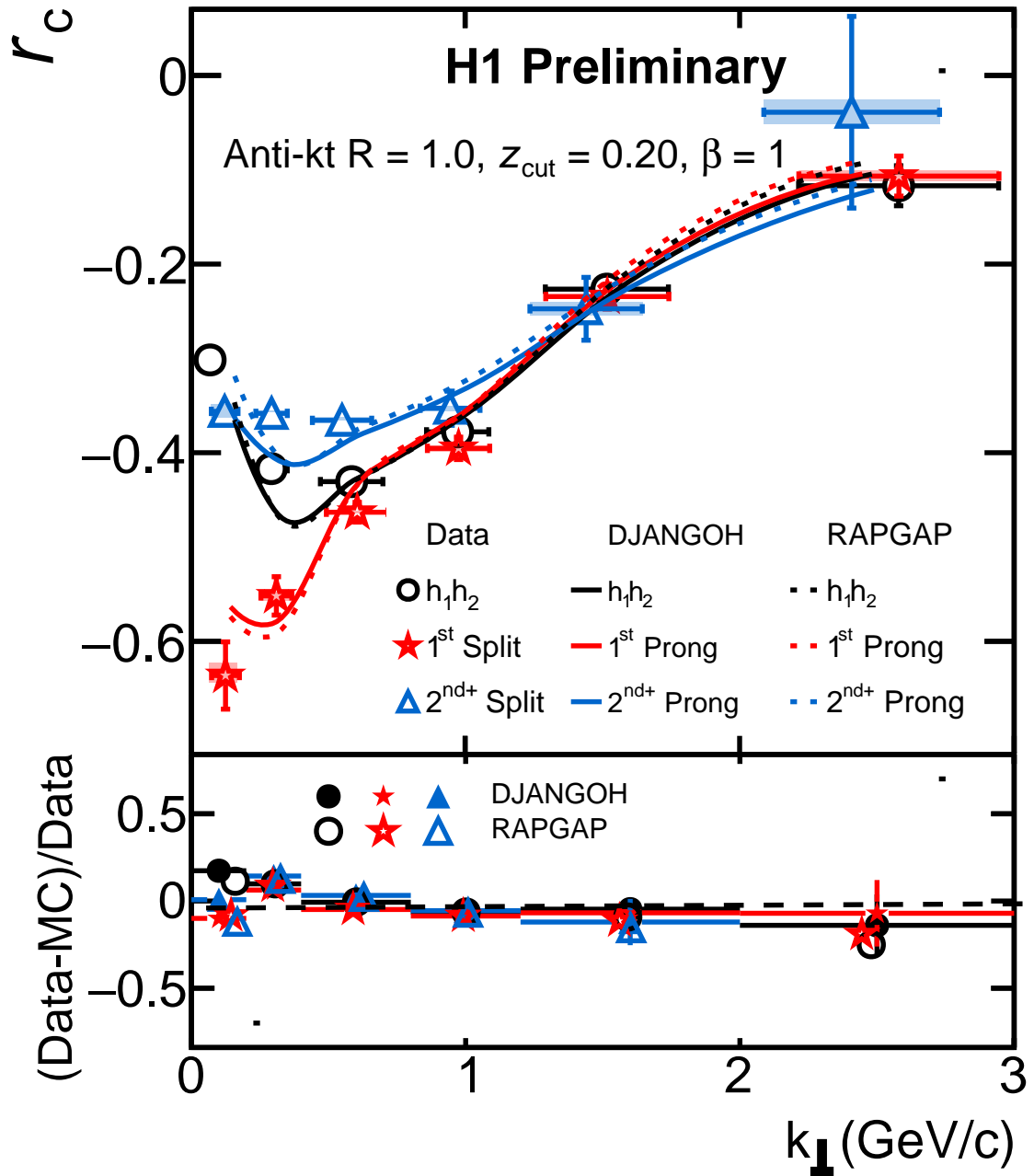


Figure 13: r_c as a function of k_{\perp} for different splits compared and $h_1 h_2$. Small k_{\perp} shows strong correlations and this is the nonperturbative region. Large k_{\perp} appears from wide angle early gluon radiations and this might trigger independent hadronization which de-correlates the r_c correlations in charge. The systematic bands are the errors appearing from bin-by-bin corrections using Rapgap and Djangoh event generators.

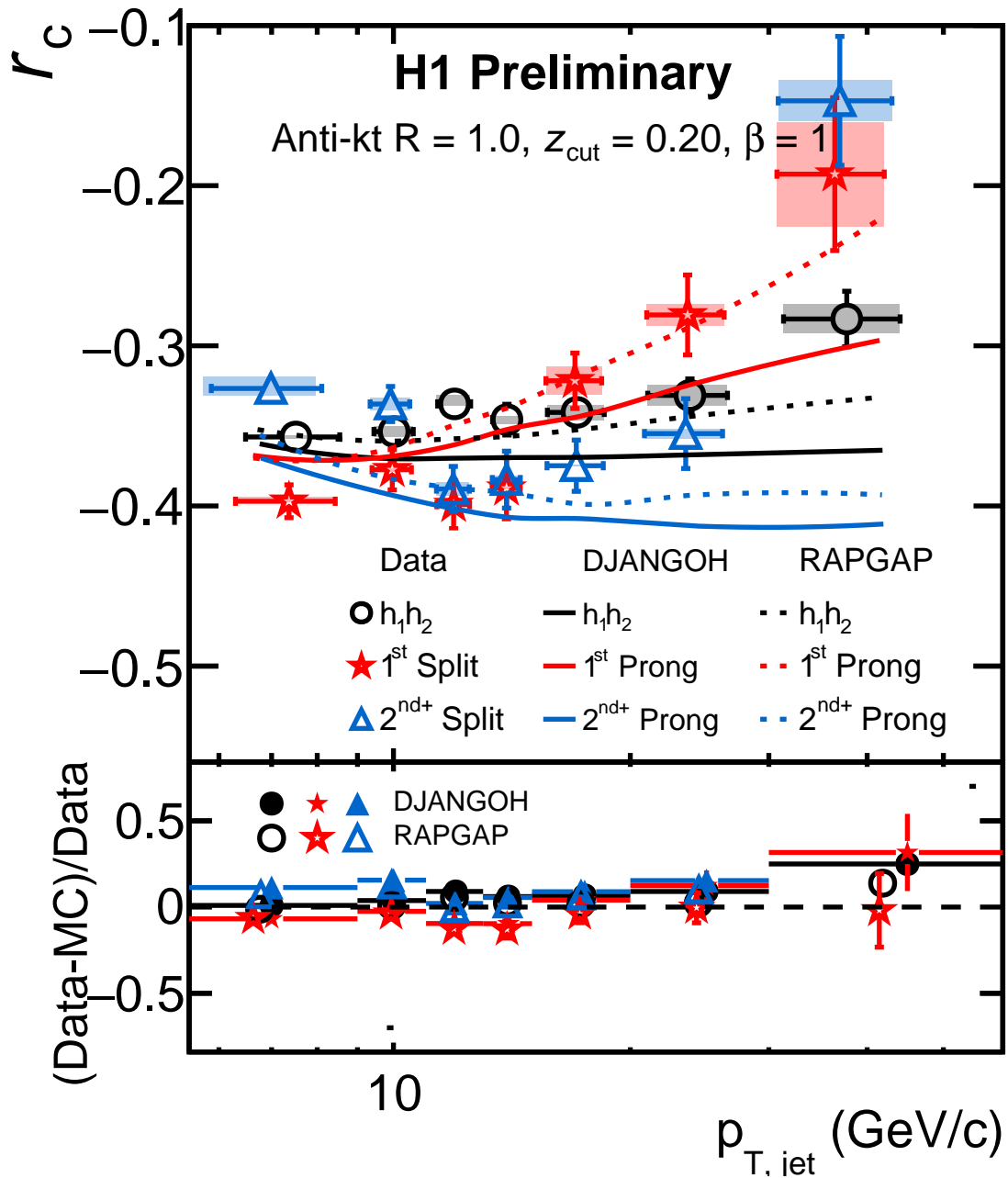


Figure 14: r_c as a function of jet transverse momentum for different splits compared with $h_1 h_2$. The r_c for $h_1 h_2$ -case depends weakly on $p_{T, \text{jet}}$. The first split seems to have stronger dependency with jet transverse momentum compared to that of the later splits. Djangoh and Rapgap comparisons are made to that with data. The systematic bands are the errors appearing from bin-by-bin corrections using Rapgap and Djangoh event generators.

References

- [1] Y. T. Chien, A. Deshpande, M. M. Mondal and G. Sterman, *Phys. Rev. D* **105**, no.5, L051502 (2022) doi:10.1103/PhysRevD.105.L051502 [arXiv:2109.15318 [hep-ph]].
- [2] A. Accardi, Y. T. Chien, D. d’Enterria, A. Deshpande, C. Dilks, P. A. G. Garcia, W. W. Jacobs, F. Krauss, S. L. Gomez and M. M. Mondal, *et al.* [arXiv:2204.02280 [hep-ex]].
- [3] R. Aaij *et al.* [LHCb], *JHEP* **09**, 006 (2013) doi:10.1007/JHEP09(2013)006 [arXiv:1306.4489 [hep-ex]].
- [4] A. J. Larkoski, S. Marzani, G. Soyez and J. Thaler, *JHEP* **05**, 146 (2014) doi:10.1007/JHEP05(2014)146 [arXiv:1402.2657 [hep-ph]].
- [5] F. A. Dreyer, L. Necib, G. Soyez and J. Thaler, *JHEP* **06**, 093 (2018) doi:10.1007/JHEP06(2018)093 [arXiv:1804.03657 [hep-ph]].